Research Article **ISSN: 2349 – 7106**

Asian Journal of Research in Chemistry and Pharmaceutical Sciences

Journal home page: www.ajrcps.com

https://doi.org/10.36673/AJRCPS.2022.v10.i02.A08

EXPERIMENTAL AND DFT STUDIES OF (*E*)-5-((4-AMINOPHENYL)DIAZENYL)-2-HYDROXYLBENZALDEHYDE AND (*E*)-N-(4-((3-FORMYL-4-HYDROXYPHENYL) DIAZENYL) PHENYL) ACETAMIDE

S. Richard Rajkumar[1], G. Rajarajan[2], V. Periyanayagasamy[1], V. Thanikachalam*[2]

[1*]Department of Chemistry, St. Joseph's College of Arts and Science (Autonomous), Tamilnadu, Cuddalore, India.

[2]Department of Chemistry, Annamalai University, Annamalainagar-608002, India.

ABSTRACT

Theoretical calculation of (*E*)-5-((4-aminophenyl) diazenyl)-2-hydroxybenzaldehyde (1) and (*E*)-N-(4-((3-formyl-4-hydroxyphenyl) diazenyl) phenyl) acetamide (2) were studied by DFTB3LYP//6-311+G (d, p) basis set. The calculated values of geometric structural parameters, FT-IR spectral data, HOMO-LUMO, NBO, NISC, Fukui function, polarizability, hyperpolarizability and UV data of compounds 1 and 2 clearly indicate that substitution on amino group alters the physical properties of the compound 2. The NICS value of amino-substituted phenyl ring reduced the aromatic character due to lone pair electron on nitrogen involved inductive, conjunction and also OH, CHO, and NH_2 and OH, CHO, and $NHCOCH_3$ in compounds (1) and (2), respectively.

KEYWORDS

HOMO-LUMO, NBO, NISC and Hyperpolarizability.

Author for Correspondence:

Thanikachalam V,

Department of Chemistry,

Annamalai University,

Annamalainagar-608002, Cuddalore, India.

Email: pvta1998@yahoo.co.in

Azo benzenes, its derivatives are used as photo responsive materials[1], dye stuffs[2], textile industries[3,4], optical data storage[5], switching technologies[6] and photo-refractive polymerindustries[7], sensitizersindye-sensitized solarcells (DSSCs) based on photosensitization of nanocrystalline titaniumdioxide(nc-TiO_2)[8], pH indicators[9], photostorage units[10], photochemical transformations[11,12], optical properties[13,14] antibacterial and pesticidal[15] antifungal, anti-diabetics, anti-neoplastics, anti-inflammatory, antiseptic and other useful chemotheraptic agents[16-18], inflammatory[19,20], anticancer and antifungal[21,22]. In this study, we report the structural geometry,

vibrational spectra, electronic absorption spectra, molecular are electrostatic potential(MEP) and NLO properties compounds 1 and 2 using the DFT calculations and to study effect of acyl group in compound 2 (Figure No.1a and No.1b).

MATERIAL AND METHODS

4-N-Acetylaminoanilide, salicylaldehyde, sodium hydroxide, sodium carbonate, sodium nitrite, and concentrated HCl were purchased from sd-fine chemicals, India. AnalaR solvents were used as such without further purifications.

General Procedure

(*E*)-N-(4-((3-Formyl-4-hydroxyphenyl) diazenyl) phenyl) acetamide [NFHPA] 2

One equivalent of 4-N-acetylaminoanilide and 1.2 equivalent sodium nitrite and conc. HCl cooled to 0^oC and added one equivalent of salicylaldehyde in 10% NaOH with constant stirring for about 1 hour. The resultant product was neutralized conc. HCl using methyl red paper. The reddish-brown product was isolated and recrystallized with ethanol. It was characterized by microanalysis. %C: 63.02(63.60); %N: 14.78(14.83)% H.4.58(4.63) and FT-IR spectrum and data are displayed in Table No.2 (Figure No.2).

Detection Method

FTIR spectrum of the compound 2 was recorded on a Bruker IFS 66V spectrometer equipped with a Globar source, Ge/KBr beams plitter and a TGS detector in the range of 4000-400cm^{-1}. The spectral resolution is ±2cm^{-1}.

The theoretical study of compounds 1 and 2 was carried out using the Gaussian 09W[23] and the output files are visualized by GaussView5.0 software[24]. The structural parameters, FTIR frequencies and HOMO-LUMO energies are calculated using B3LYP methods with a 6-311+G (d, p) basis set. The vibration frequencies are obtained by the DFT method and are scaled-down by using scaling factors 0.961 and 0.958[25]. The vibrational assignments of compounds 1 and 2 are using the Veda-4 program[26]. The NBO analysis was performed by utilizing NBO3.1 program in the Gaussian09W at B3LYP/6-311+G (d, p) method. To investigate the reactive sites (charged region of a molecule), molecular electrostatic potential (MEP) were evaluated using the above method.

RESULTS AND DISCUSSION

Optimized Parameters

The optimized structural parameters of compounds 1 and 2 are calculated by DFT-B3LYP level with 6-311+G (d, p) basis sets and data are compiled in Table-S1 in accordance with the atomic numbering scheme given in Figure No.1a and No.1b and data were compared with the experimental values[27].

The computed C-C bond lengths of phenylring vary between1.386 and 1.418Å. However, the optimized C-C bond for the aromatic system is invariably 1.386-1.401Å. In the present study, the computed C-N bonds are in the range 1.411-1.454 Å and their XRD values are in the range of 1.368-1.3776Å[27,28]. The optimized N-N bond distance is 1.257 Å and their experimental value is 1.237 Å. The optimized N-H bonddistancesrangefrom1.008-1.012Å for 1 and 1.012 Å for 2, the data are comparable with the experimental value of 0.820-0.852 Å and 0.903 Å, respectively. The optimized C-H bond lengths vary from 1.081-1.086 Å and its experimental value is 0.93Å. The theoretical bond angles of C-C-C, C-C-Hand C-N-N, C-N-H and C-C-O range from 118.4-125.1º which are comparable with the experimental values[27]. The theoretical dihedral angles for the title molecules are given in Table-S1. The values are clearly indicate that phenyl rings, aldehyde and amine are planar with respect to the AZO group and *trans* configuration of two phenylrings[29].

FTIR Frequencies Analysis

Theoretical study of compounds 1, 2 using Gaussian 09 window program package and experimental study of compound 2. Geometrical optimization, vibrational frequency and other parameters were performed by B3LYP/ 6-311+ G (d, p) level of DFT Table No.1 and Table No.2 (Figure No.2). The total energy distributions were calculated for the assignment of frequencies using VEDA 4 software[26].

It is more sensitive to hydrogen bonding and non-hydrogen bonded free OH observed in 3550 to 3700 cm^{-1} region, Table No.1 and Table No.2 (Figure No.2). The intra-molecular hydrogen bonding could

also be present could reduce the OH stretching frequency band in 3200 to 3500 cm^{-1}. The title molecule OH theoretical stretching mode is assigned at 3281 cm^{-1} (mode no.3) 3292 cm^{-1} (mode no.1) FTIR. The band at 1537, 1361, 1298 (modeno.16, 23 and 26 for 1), 1485, 1298, (mode no.19, 31 for 2) experimental value at 1274 are assigned to bending vibration of phenolic group.

For the title compounds N-H (not for 1) stretching mode is not observed, the theoretical values of N-H stretching are observed at 3567, 3465 (Mode No.1, 2) and 3275 (Mode No.2) with experimental value 3181 cm^{-130}. The bending vibration of NH group observed at 1361 and 1302 cm^{-1}, respectively.

C-H Stretching frequency

Some characteristics of bands of the stretching vibration of CH aliphatic and CH aromatic, the C-H aromatic stretching modes were observed from 3109 to 3067 cm^{-1} (theoretical) 3133 and 3067 cm^{-1}, (experimental) in IR spectra of compound 2. The C-H in-plane bending vibrations were observed within in the region 1000 to1300 cm^{-1} (mode no. 35-37 for 1 and 33-44 for 2), showing good agreement with the experimentally observed values[31].

C=O Stretching frequency

The carbonyl stretching vibrations of FTIR spectra and theoretical values are listed in Table No.1 and No.2, it gives an intense FTIR absorption band due to different electro negativity distributed between two atoms. The absorption band of the carbonyl group and amide group of oxygen is decided by electron density on oxygen. The strong band observed at 1655 cm^{-1} in FTIR assigned to C=O of carbonyl also amide and theoretical values are 1668 and 1628 cm^{-1} (modeno.14) and it's further supported by TED value 79% and 71%, respectively. In-plane bending aldehyde, frequency are observed at 1335(56 %) and amide frequencies at 1516 with 26% of TED.

N=N and C-N group stretching frequency

The title compound possesses two bands wise C-N=N the stretching vibration has very characteristic and intense band IR due to asymmetric nature. The reported data reveal that bands occurring at 1425 cm^{-1}, the C-N mode AZO compound are expected to appearing the region 1200 to 1300 cm^{-1}. The frequency and intensity depending upon the neighboring group effect due to amide, hydroxyl and aldehyde. A strong band appears at 1475 cm^{-1} (FTIR) originating from stretching vibration bands are assigned to νN10-N11. These assignments are in coincidence with the frequency value of 1184 and 1263 cm^{-1}.

Mulliken and natural population analysis

Mulliken atomic charges of compounds 1 and 2 are calculated at B3LYP level and displayed in Table No.3. The amount of the charges are calculated on N10, N11, N22 for compound 1 0.0323, 0.0802, -0.3603 and N10, N11, N27 for compound 2 0.0483, 0.0857 and -0.1937, the values are found to be N10, N11 are positive whereas N22 and N27 compounds 1 and 2 are negative values. The greater negative charge of N22 indicates that the lone pair involved in conjugation which is further supported by the greater electron density on C19 carbon that is -0.1347 and on C17 carbon -0.2205. The C20 and C21 ring hydrogen less positive when compared with the compound 2, which indicates that hyper conjugation effect in compound 1, which is further supported (atomic charge is -0.205 at C17 in 1 and is 0.1813 at C17 in 2, Table No.3). The charge distribution data show that the double bond character of carbon atoms are negative except C1, C4, C15 in compound 1 and C1, C4, C17, C19 in compound 2. In compound 1, H20 and H22 are less positive in comparison with the compound 2. The N atom in compound 1(amino group) more negative whereas all H atoms are more positive due to less electro negativity of carbon bonded hydrogen atoms.

NBO analysis

NBO calculations were performed using the Gaussian09W package at B3LYP//6-311+G (d, p) the DFT level Table No.S2 and Table No.S3 in order to understand various second-order interactions between the filled orbital of second-order and vacant orbital of another system, donor-acceptor assure of intra-molecular delocalization or hyper-conjugation results[32].

Second order Fock matrix was carried out to evaluate on or acceptor interaction in natural bond orbital basis. The interaction result in a loss of

occupancy from the localized NBO of the idealized Lewis structure into on empty non- Lewis orbital. For each donor i and acceptor j the stabilization energy E^2 associated with the delocalization it jis determined $E^2 = \Delta E_{ij}$ qi is the donor orbitals occupancy and E_i and E_j are diagonal elements and F(i,j) is the off-diagonal.

The calculated perturbation energy of the significant donor-acceptor values of compound 1 and 2 are presented in Table No.S2 and Table No.S3. The greater intra-molecular hyper conjugative interaction of π*and π*of anti-bonding of C-C to anti-bonding of C-C bond of the aromatic rings results to the stabilization of a few parts of the ring as evident from Table No.S2 and Table No.S3. The best value results to strong delocalization of 139.31kcal mol^{-1} *C4-C5 to *C1-C6,155.34 kcal mol^{-1} *C4-C5to*C2-C3,242.63kcal mol^{-1}, *C15-C19 to *C14-C17, 128.73kcal mol^{-1} compound 1 and 133.13kcal mol^{-1} *C4-C5 to *C1-C6,168.15 kcal mol^{-1}* C4-C5to*C2-C3, 255.37kcal mol^{-1},*C15-C19 to *C14-C17, 145.13kcalmol^{-1}* C24-O26 to *C4-C5, 475.80kcal mol^{-1} LP(3) O22 to LP*(1) H23 correspondingly. The data indicate that the existing of intra-molecular hydrogen bonding between carbonyl group and hydrogen atoms of compounds 1 and 2, respectively.

Molecular electrostatic potential (MEP)

Molecular electrostatic potential data are to understanding the charge density, and polarity of the studied compounds 1 and 2. From the colour region of the compounds 1 and 2, (Figure No.4) Red colour due to the maximum negative potential region, the blue colour due to the maximum positive potential region and green due to the zero potential areas[33]. Nitrogen atom N22 in compound 1 and N27 in compound 2 nucleophilic attack regions because of its maximum negative potential. Mesmeric effect of amino group represents within the area with large electronic charge indicates reddish yellow colour. However, the hydrogens H7, H8, H9, H16, H18, H20, H21, H23, H24, H26 and H28 represents large positive potential surface and results to an electrophilic attack region with a blue shade surrounding, electrons within the benzene ring are proven the greenish shade of the molecule and similar data were observed in compound 2, respectively.

Aromaticity

Aromaticity of compounds 1 and 2 are determined by theoretically usingB3LYP/ 6-311+ G (d, p) basis set of DFT method and values are listed in Table No.S4. This model is predicted on the subsequent equation[33].

HOMA = $1-[(\frac{\alpha}{n}\sum R_{opt} - R_i)^2]$

= $1-\alpha(R_{opt}-R_i)^2-(\frac{\alpha}{n})\sum(R_{av} - R_i)^2$

= 1-EN-GEO

Where α (ie = 257.7) is an empirical constant that is fixed so that aromatic compounds (where all bonds equal R_{opt} =1.388) and R_i is the individual bond lengths. Since both the EN and GEO terms are dearomatization terms, an increase or decreases in either term the degree of aromaticity. EN terms the difference between the mean bond length and the optimal bond length, and the GEO terms the degree of bond alternation. The bond lengths used in this calculation can be computed or measured experimentally.

In compound 1, NISC value is somewhat lower than anilide ring (Tables No.S5 and No.S6) which indicates that absence of conjugation in the benzene ring. Anion and cation states are less aromatic characters than neutral state in compounds 1 and 2. This was further supported by HOMA values (Tables S7 and No.S8). This implies that reducing of both central bond lengths in the benzene ring as a result of substituent cooperative interactions may be considered in these studied compounds main cause of the lower values of aromatic character observed with an increase of the π-electron cooperative effects between the substituents. The NICS values of phenol and aniline are 0.742 and 0.923, respectively. As can seen from Fukki function[34,35] data in Tables No.S7 and No.S8, the order of electrophilicity sites of compound 1 is C6>C4>C2>C12.>C3>C17 and C15>C2>C12> C4>C13>C3>C14 for compound 2. Furthermore the order of nucleophilicity sites of compound 1is C15>C13>C14>C19>C27>C5>C1 and C6>C29>C24>C1>C5>C17>C19 for compound 2,

respectively. Acyl substituent in compound 2 alter the electrophilicity and nucleophilicity sites.

NLO property

The average polarizability (α_0) , anisotropy polarizabilty (Δα), dipole moment (μ), and hyperpolarizablity (β_0) of compounds 1 and 2 are calculated using the following equations.

$\mu = (\mu_x^2 + \mu_y^2 + \mu_z^2)^{1/2}$

$\alpha_0 = (\frac{\alpha_{xx}+\alpha_{yy}+\alpha_{zz}}{3})$

$\Delta\alpha = \frac{1}{\sqrt{2}}((\alpha_{xx}- \alpha_{yy})^2 + (\alpha_{yy}- \alpha_{zz})^2 + (\alpha_{zz}- \alpha_{xx})^2 + 6(\alpha_{xy}^2 + \alpha_{yz}^2 + \alpha_{zx}^2))^{1/2}$

$\beta_0 = (\beta_x^2 + \beta_y^2 + \beta_z^2)^{1/2}$

$\beta_x = \beta_{xxx} + \beta_{xxy} + \beta_{xxz}$

$\beta_y = \beta_{yyy} + \beta_{yyx} + \beta_{yyz}$

$\beta_z = \beta_{zzz} + \beta_{zzy} + \beta_{zz}$

The calculated values of average polarizability, anisotropy polarizabilty, dipole moment, and hyperpolarizablity of compound 1 and 2 are summarised in Table No.5[36]. The anisotropy polarisabilty and first hyperpolarisability values of compounds 1 and 2 are 4.39x 10^{-24}, 8.40 x 10^{-24} and 3.44 x 10^{-30} and 1.83 x 10^{-30} esu, respectively and are compiled in Table No.5. In which, the β value of 1 and 2 are nine and five times greater than that of urea. The dipole moment and energy of compounds 1 and 2 various with dihedral angle and shown in Figure No.S1 and No.S2 (atoms 1, 2, 10, 11, Figure No.1a and No.1b) maximum values are occurred at 100^o and -100^o for both studied compounds, respectively. This shows that the molecules 1 and 2 have good NLO property.

FMO analysis

The HOMO and LUMO energies calculated by B3LYP method is shown below. This electronic absorption corresponds to the transition from the ground to the third excited state and is mainly described by one electron excitation from the highest occupied molecular orbital (HOMO) to the lowest unoccupied molecular orbital (LUMO). Energy difference between HOMO and LUMO analysis is named as energy gap that's is a crucial stability of the structures (Table No.4; Figure No.3). The HOMO is found over the AZO nitrogen atoms near and ring carbons, the HOMO → LUMO transition implies that an electron density transfer to AZO groups to phenyl group (phenolic and aldehyde substituent's and HOMO-1 to LUMO transition takes place from whole molecule in compound 1, similar trends are also observed in compound 2. The atomic orbital compositions of the FMO are shown in Figure No.4. The energy cap values are small which indicate that intra-molecular transition happen in these compounds and are more soft characters[37,38].

UV-visible data

The UV-vis absorption spectra of the compound 2 in various dielectric solvents is shown in Figure No.S3. On the idea of fully optimized ground-state structure, TD-DFT/B3LYP/6-311G+(d,p) calculations are wont to determine the low-lying excited theoretical states of compounds 1 and 2. The obtained results involving the vertical excitation energies, oscillator strength (f) and wavelength are measured and therefore the results are compared with the experimental wavelength. These values are varied from 358-361 nm (f = 0.701-0.7292) and 398-400 nm (f = 0.9623 – 1.001) due to polarity of the solvents used for compound 1 and for compound 2, respectively and transitions were assigned to n-π* and internal charge transfer spectra[39] (Table No.S9 and No.S10).

Thermodynamic properties

Thermodynamic parameters such as zero-point vibrational energy (ZPVE) and entropy, $S_{vib}(T)$ compounds 1 and 2 are presented in Table No.6.

The variation in ZPVE seems to be insignificant. Entropy of compounds 1 and 2 at temperature are summarized in Table No.6. The ZPVE values of compound 2 is more negative compared with compound 1 and thermodynamically more stable than that of compound 1.

Table No.1: Vibrational wave numbers obtained for compound 1 DFT-B3LYP/6-311+G (d, p) [harmonic frequency (cm^{-1}), IR intensity, Raman activity (Km/mol), reduced masses (amu) and force constants ($mDyneA^{\circ -1}$)]

Mode No	Calculated frequencies (cm^{-1})	IR intensity	Raman activity	Reduced mass	Force constant	Vibrational assignments WITH >10 % PED
1	3567	24.0243	99.7496	1.101	8.8282	ν N22-H23 (100)
2	3465	94.9698	747.8021	1.0467	7.9252	ν N22-H24 (100)
3	3281	373.7357	195.3549	1.0681	7.2471	ν O25-H26 (99)
4	3103	4.2303	70.9613	1.093	6.6319	ν C1-H7 (87) + ν C6-H9 (12)
5	3101	2.7189	36.5691	1.0918	6.6169	ν C14-H18 (97)
6	3084	6.681	102.5539	1.0934	6.5584	ν C13-H16 (91)
7	3083	3.6636	159.3096	1.0895	6.5312	ν C1-H7 (12) + ν C6-H9 (87)
8	3069	1.5374	36.082	1.0904	6.4744	ν C3-H8 (99)
9	3058	22.3715	172.4363	1.0887	6.4197	ν C15-H20 (91)
10	3053	23.0291	161.3399	1.0895	6.4005	ν C17-H21 (97)
11	2855	75.9881	111.568	1.086	5.5801	ν C27-H28 (99)
12	1625	648.7798	101.0901	7.4306	12.6894	ν O29-C27 (69)
13	1588	311.7707	428.3661	1.6116	2.6287	β H24-N22-H23 (57)
14	1583	160.8943	344.5353	4.1635	6.7452	ν C3-C2 (25) + ν C1-C2 (14) + β H24-N22-H23 (10)
15	1571	214.4179	160.3707	3.1019	4.947	ν C13-C12 (16) + ν C14-C12 (18) + β H24-N22-H23 (18)
16	1537	47.5766	76.0974	4.4543	6.8076	ν C17-C14 (12) + ν C1-C2 (14) + β H26-O25-C5 (11)
17	1533	79.1858	119.1443	5.1021	7.7593	ν C17-C14 (35) + β C19-C15-C13 (10)
18	1473	88.4474	1793.607	3.6376	5.1127	ν N10-N11 (28) + β H21-C17-C14 (10)
19	1453	58.5319	3025.15	3.4003	4.6423	ν N10-N11 (20) + β H7-C1-C6 (14)
20	1424	96.1593	3940.029	3.0772	4.0381	ν N10-N11 (13) + β H7-C1-C6 (23)
21	1404	13.745	429.5188	3.6312	4.6278	ν C15-C13 (31)
22	1398	52.3431	4166.465	3.9788	5.0251	ν N10-N11 (20) + ν C4-C3 (14)
23	1361	84.2318	56.1912	1.9005	2.2752	ν C6-C1 (17) + β H26-O25-C5 (34) + β H26-C27-O29 (23)
24	1333	56.2424	445.3182	1.7383	1.9982	ν C6-C1 (14) + β H26-C27-O29 (53)
25	1302	4.0329	46.4637	4.9148	5.3838	ν C13-C12 (27) + ν C14-C12 (10) + ν C19-C15 (14) + β H23-N22-C19 (13)
26	1298	55.2828	59.5932	2.8405	3.0945	ν C6-C1 (14) + ν C4-C3 (10) + β H26-O25-C5 (14)
27	1271	0.0644	403.7214	1.5173	1.5849	β H18-C14-C17 (52)
28	1256	24.9921	58.1528	3.2745	3.3407	ν O25-C5 (15) + ν N22-C19 (31) + β H8-C3-C4 (12)
29	1253	406.6518	213.3074	3.6059	3.6615	ν O25-C5 (29) + ν N22-C19 (18) + β H7-C1-C6 (12)
30	1216	27.3022	247.0962	2.8118	2.6851	ν C3-C2 (12) + ν N11-C12 (31) + β H8-C3-C4 (14)
31	1190	83.3059	1746.119	2.2593	2.0676	ν C4-C3 (11) + ν N11-C12 (10) + ν N10-

						C2 (15) + β H21-C17-C14 (19)
32	1164	76.4211	1204.557	2.3208	2.0322	ν C5-C6 (37) + β H16-C13-C15 (12)
33	1121	177.2546	141.135	1.3317	1.0832	β H7-C1-C6 (15) + β H21-C17-C14 (29)
34	1108	83.6809	2451.632	1.5534	1.2329	ν N10-C2 (16) + β H9-C6-C1 (45)
35	1093	10.8765	7.1241	1.1813	0.913	β H23-N22-C19 (12) + β H20-C15-C13 (48)
36	1074	27.094	1459.36	1.5701	1.1715	β H16-C13-C15 (33)
37	1018	3.6994	7.4812	1.4269	0.9566	β H23-N22-C19 (57)
38	975	1.8459	1.1716	1.693	1.0411	τ H28-C27-C4-C3 (76)
39	971	0.8872	19.1109	2.5578	1.5611	β C6-C1-C2 (12) + β C17-C14-C12 (39) + β C15-C13-C12 (13) + β C4-C3-C2 (11)
40	954	0.0979	0.0599	1.3184	0.7766	τ H9-C6-C1-C2 (35) + τ H16-C13-C15-C19 (42)
41	939	0.1771	0.0509	1.3248	0.7551	τ H18-C14-C17-C19 (61) + τ H20-C15-C19-N22 (16)
42	921	4.0883	4.6961	3.7544	2.06	ν C5-C6 (20) + β C4-C3-C2 (16)
43	920	1.6984	0.4777	1.3252	0.7262	τ H16-C13-C15-C19 (10) + τ H18-C14-C17-C19 (12) + τ C19-C15-C13-C12 (18)
44	878	1.959	13.154	7.1394	3.5525	ν C19-C15 (23) + β N10-N11-C12 (12) + β C2-N10-N11 (16)
45	875	19.049	0.5717	1.4275	0.7064	τ H7-C1-C6-C5 (11) + τ H8-C3-C4-C5 (25) + τ C16-C13-C15-C19 (12) + τ C5-C6-C1-C2 (14)
46	820	18.2619	0.0283	1.4591	0.6349	τ H7-C1-C6-C5 (20) + τ H8-C3-C4-C5 (26)
47	809	35.9859	31.4479	2.2713	0.9617	τ H20-C15-C19-N22 (18)
48	806	17.2222	64.1027	3.2613	1.369	ν C19-C15 (15) + τ H20-C15-C19-N22 (19)
49	782	0.7124	0.1637	1.2618	0.4998	τ H21-C17-C19-N22 (27)
50	773	33.3217	4.9062	5.1673	1.9979	β C19-C15-C13 (11) + β C14-C12-C13 (10)
51	780	117.7131	1.2078	1.1052	0.413	τ H26-O25-C5-C4 (87)
52	743	16.1172	60.9457	5.141	1.8337	ν C27-C4 (27) + β C5-C6-C1 (11) + β C1-C2-N10 (16)
53	699	2.3122	0.5379	4.3403	1.3717	τ C19-C15-C13-C12 (10) + Γ N22-C15-C17-C19 (25) + Γ N11-C13-C14-C12 (12)
54	681	0.7282	2.0356	4.6249	1.3873	τ H9-C6-C1-C2 (12) + τ C6-C1-C2-N10 (11) + τ C5-C6-C1-C2 (13) + Γ O25-C4-C6-C5 (28)
55	676	36.5188	0.5362	6.3005	1.8624	β O29-C27-C4 (22) + β C6-C1-C2 (11)
56	623	0.8642	9.5307	6.9018	1.7357	ν C17-C14 (11) + β C19-C15-C13 (11) + β C15-C13-C12 (11) + β C14-C12-C13 (22)
57	601	4.8016	35.1807	6.8806	1.6109	β C17-C14-C12 (12) + β C4-C3-C2 (10)

58	563	19.0465	0.2966	2.7766	0.5694	τ C2-N10-N11-C12 (16) + Γ O25-C4-C6-C5 (16) + Γ C27-C3-C5-C4 (11) + Γ C3-C1-N10-C2 (20)
59	516	1.9794	5.4906	5.7431	0.9909	β C6-C1-C2 (14) + β C3-C2-N10 (18) + β N11-C12-C14 (17) + β C2-N10-N11 (11)
60	501	12.719	4.644	2.417	0.3932	Γ N22-C15-C17-C19 (37) + Γ N11-C13-C14-C12 (16)
61	463	13.7857	3.7271	5.1385	0.7126	β C17-C14-C12 (17) + τ H23-N22-C19-C15 (11)
62	443	5.4267	8.3703	6.2825	0.7972	β O29-C27-C4 (20) + β O25-C5-C6 (43)
63	432	339.675	86.2574	2.105	0.255	τ H23-N22-C19-C15 (46)
64	429	126.8454	26.6752	2.8373	0.3376	τ H23-N22-C19-C15 (16) + τ H16-C13-C15-C19 (11) + τ C4-C3-C2-C1 (25)
65	413	68.2106	14.9134	2.7671	0.3058	τ C17-C14-C12-C13 (33) + τ C5-C6-C1-C2 (10)
66	400	27.4855	2.7056	4.8068	0.498	β C15-C13-C12 (12) + β O25-C5-C6 (11) + β N22-C19-C17 (18)
67	385	32.4341	5.2942	3.7909	0.3659	τ C6-C1-C2-N10 (21) + τ C17-C14-C12-C13 (18) + τ C4-C3-C2-C1 (10) + τ C2-N10-N11-C12 (11)
68	359	13.0931	1.3269	3.7887	0.3166	β O25-C5-C6 (10) + β N22-C19-C17 (48)
69	341	6.064	4.9615	5.3815	0.405	τ C5-C6-C1-C2 (11) + Γ C3-C1-N10-C2 (22) + Γ N11-C13-C14-C12 (23)
70	325	14.3892	0.2628	1.0371	0.0713	τ H24-N22-C19-C15 (43)
71	277	3.6598	0.7064	2.7811	0.1386	τ H28-C27-C4-C3 (11) + τ O29-C27-C4-C3 (27) + Γ O25-C4-C6-C5 (10) + Γ C27-C3-C5-C4 (35)
72	276	7.1642	0.3011	6.47	0.3197	β O29-C27-C4 (14) + β C27-C4-C5 (36)
73	209	4.7181	5.1291	6.8152	0.1928	ν C4-C3 (11) + ν N10-C2 (18) + β C27-C4-C5 (27)
74	185	3.2407	0.1029	6.8213	0.1701	τ N10-N11-C12-C13 (28) + τ C17-C14-C12-C13 (13) + τ C1-C2-N10-N11 (19)
75	180	2.6603	0.233	5.6317	0.1193	τ O29-C27-C4-C3 (15) + τ C15-C13-C12-C14 (29) + τ C2-N10-N11-C12 (15) + Γ C3-C1-N10-C2 (10)
76	176	1.4654	3.689	6.4651	0.1316	ν N10-C2 (10) + β N10-N11-C12 (10) + β C3-C2-N10 (20) + β N11-C12-C14 (26)
77	134	0.0058	0.9197	6.5246	0.0776	τ O29-C27-C4-C3 (25) + τ C15-C13-C12-C14 (11) + Γ C27-C3-C5-C4 (27) + Γ C3-C1-N10-C2 (13)
78	82	2.7625	1.0841	6.1327	0.027	τ N10-N11-C12-C13 (25) + τ C6-C1-C2-N10 (21) + τ C5-C6-C1-C2 (10) + τ C19-C15-C13-C12 (10)
79	55	1.2312	1.7146	6.1359	0.0125	β N10-N11-C12 (29) + β C3-C2-N10 (20) + β N11-C12-C14 (15) + β C2-

						N10-N11 (28)
80	40	0.3953	0.5448	6.5488	0.0068	τ C15-C13-C12-C14 (22) + τ C2-N10-N11-C12 (39) + Γ N11-C13-C14-C12 (18)
81	24	0.2558	0.5913	4.1096	0.0016	τ N10-N11-C12-C13 (38) + τ C1-C2-N10-N11 (54)

Table No.2: Vibrational wave numbers obtained for compound 2 DFT-B3LYP/6-311+G (d, p) [harmonic frequency (cm^{-1}), IR intensity, Raman activity (Km/mol), reduced masses (amu) and force constants ($mDyneA°^{-1}$)]

Mode No	Experimental frequencies (cm^{-1})FT IR	Calculated frequencies (cm^{-1})	IR intensity	Raman activity	Reduced mass	Force constant	Vibrational assignments WITH >10 % PED
1	3292	3458	394.23	252.05	1.07	7.22	ν O22-H23 (99)
2	3191	3275	45.23	361.58	1.08	8.1	ν N27-H28 (100)
3	3133	3109	7.5	81.93	1.09	6.66	ν C14-H18 (52) + ν C17-H21 (47)
4		3104	3.95	76.24	1.09	6.64	ν C1-H7 (87) + ν C6-H9 (12)
5		3096	3.04	47.93	1.09	6.57	ν C14-H18 (47) + ν C17-H21 (52)
6		3088	4.51	98.52	1.09	6.57	ν C13-H16 (86) + ν C15-H20 (12)
7		3086	2.73	160.96	1.09	6.54	ν C1-H7 (12) + ν C6-H9 (87)
8	3067	3070	0.99	34.21	1.09	6.48	ν C3-H8 (99)
9		3067	12.77	118.5	1.09	6.46	ν C13-H16 (12) + ν C15-H20 (88)
10		3043	10.92	93.1	1.1	6.44	ν C31-H32 (30) + ν C31-H34 (69)
11		3010	6.12	67.26	1.1	6.26	ν C31-H32 (44) + ν C31-H33 (42) + ν C31-H34 (14)
12		2946	2.37	188.75	1.04	5.68	ν C31-H32 (26) + ν C31-H33 (57) + ν C31-H34 (16)
13	2858	2858	71.62	107.92	1.09	5.59	ν C24-H25 (99)
14	1655	1668	710.46	200.33	7.33	13.19	ν O30-C29 (79)
15		1628	746.56	114.16	7.61	13.04	ν O26-C24 (71)
16	1591	1584	83.79	638.75	6.44	10.43	ν C2-C3 (15) + ν C4-C3 (15) + ν C5-C6 (20)
17	1537	1570	301.62	1179.5	6.11	9.73	ν C15-C13 (12) + ν C17-C14 (24) + ν C13-C12 (13)
18	1487	1491	2.42	6.16	5.72	8.79	ν C19-C15 (17) + ν C13-C12 (21)
19		1485	141.75	34.45	3.97	6.05	ν C1-C2 (16) + β H23-O22-C5 (14)
20		1475	42.78	4409.2	3.92	5.52	ν N10-N11 (34) + β H21-C17-C19 (12)
21		1455	170.44	3695.32	3.24	4.43	ν N10-N11 (18) + β H18-C14-C17 (12)
22		1429	45.52	228.38	2.03	2.68	β H28-N27-C29 (33) + β H20-C15-C19(14)
23	1401	1425	26.53	5300.92	2.71	3.56	ν N10-N11 (18) + β H7-C1-C2 (12) + β H9-C6-C1 (11)
24		1356	10.72	478.6	1.15	1.49	β H32-C31-H34 (34) + β H34-C31-H33 (29) + τ H34-C31-C29-N27 (15)

25		1409	25.5	3.02	1.06	1.36	β H32-C31-H34 (24) + β H33-C31-H32 (48) + τ H32-C31-C29-N27 (10)
26		1402	1.57	1618.64	4.19	5.32	ν C4-C3 (19)
27	1371	1368	6.79	1242.09	2.61	3.16	ν C15-C13 (13) + ν C17-C14 (18) + β H16-C13-C15 (11) + β H28-N27-C29 (18)
28		1360	86.64	125.25	2.01	2.41	ν C1-C6 (15) + β H25-C24-O26 (19) + β H23-O22-C5 (34)
29	1311	1338	104.21	39.88	1.33	1.54	β H32-C31-H34 (14) + β H33-C31-H32 (32) + β H34-C31-H33 (37)
30		1335	76.04	522.86	1.68	1.93	ν C1-C6 (10) +β H25-C24-O26 (56)
31	1274	1298	56.06	16.52	2.72	2.96	ν C3-C2 (15) + β C1-C2-N10 (10) + β H23-O22-C5 (12)
32		1278	62.12	1051.08	4.74	5	ν C14-C12 (23) + ν C19-C15 (17)
33		1268	4.06	17.34	1.64	1.71	β H21-C17-C19 (21) + β H18-C14-C17 (20) + β H16-C13-C15 (11) + β H20-C15-C19(10)
34		1263	437.57	179.82	2.97	3.06	ν N27-C29 (32)
35		1258	557.54	210.64	3.7	3.78	ν O22-C5 (37) + β H7-C1-C2 (13)
36		1217	24.68	278.57	2.82	2.7	ν C4-C3 (10) + ν N10-C2 (20) + β H8-C3-C2 (13) + β H9-C6-C1 (11)
37		1194	32.37	589.84	2.66	2.45	ν C17-C14 (10) + ν C19-C15 (16) + ν N27-C19 (19)
38		1184	35.93	1368.47	2.11	1.92	ν N11-C12 (24) + β H8-C3-C2 (10) +β H20-C15-C19(14)
39	1154	1162	110.43	1403.52	2.27	1.98	ν C5-C6 (28) + ν C24-C4 (10) + β H9-C6-C1 (12)
40		1125	122.99	730.3	1.37	1.12	β H18-C14-C17 (17) + β H16-C13-C15 (13)
41	1103	1110	32.67	3516.69	1.59	1.26	β H7-C1-C2 (10) + β H9-C6-C1 (14) + β H8-C3-C2 (11)
42		1083	7.48	51.44	1.29	0.97	ν C15-C13 (14) + β H20-C15-C19(10) + β H16-C13-C15 (19) + β H18-C14-C17 (17)
43	1014	1073	66.56	1739.81	1.6	1.19	β H7-C1-C2 (29) + β H8-C3-C2 (10)
44		1007	10.76	4.5	1.74	1.14	β H32-C31-H34 (17) + τ H32-C31-C29-N27 (36) + τ H34-C31-C29-N27 (15) + γ O30-C31-N27-C29 (19)
45		982	72.54	3.38	1.59	0.99	β H33-C31-H32 (10) + β H34-C31-H33 (11) + τ H32-C31-C29-N27 (11) + τ H33-C31-C29-N27 (29) + τ H34-C31-C29-N27 (10)

46	966	978	0.45	15.04	2.51	1.55	β C15-C13-C12 (23) + β C17-C14-C12 (32) + β C14-C12-C13 (12)
47		955	1.94	1.23	1.69	1.04	τ H25-C24-C4-C3 (75)
48		954	0.1	0.08	1.32	0.78	τ H7-C1-C2-C3 (56) + τ H9-C6-C1-C2 (22)
49		929	0.3	3.31	1.33	0.77	τ H18-C14-C17-C19 (41) + τ H21-C17-C19-N27 (30) + τ C17-C14-C12-C13 (10)
50	901	921	0.51	0.88	1.34	0.75	τ H16-C13-C15-C19 (31) + τ H20-C15-C19-N27 (22) + τ C15-C13-C12-C14 (11) + τ C19-C15-C13-C12 (19)
51		883	4.68	5.73	3.75	2.06	ν C1-C2 (24) + β C6-C1-C2 (14)
52		878	5.64	26.75	4.61	2.33	ν C14-C12 (12) + ν C31-C29 (10) + β C14-C12-C13 (12)
53	835	877	3.13	9.4	5.16	2.57	ν C14-C12 (12) + β N10-N11-C12 (11) + β C19-C15-C13 (10) +β N10-N11-C12 (11) + β C2-N10-N11 (14)
54		826	19.43	0.58	1.47	0.73	τ H8-C3-C2-C3 (70)+ γ C3-C1-N10-C2 (12)
55		819	54.15	3.2	1.68	0.74	τ H18-C14-C17-C19 (12) + τ H20-C15-C19-N27 (20) + τ H21-C17-C19-N27 (25)
56		797	0.38	0.42	1.47	0.64	τ H7-C1-C2-C3 (14) + τ H9-C6-C1-C2 (48) + γ O22-C4-C6-C5 (11)
57		763	2.06	6.24	1.37	0.56	τ H16-C13-C15-C19 (23) + τ H18-C14-C17-C19 (14) + τ H20-C15-C19-N27 (33) + τ H21-C17-C19-N27 (19)
58		758	120.32	1.29	1.11	0.42	τ H23-O22-C5-C4 (86)
59	737	743	1.22	7.2	4.28	1.59	ν C31-C29 (32) + β C14-C12-C13 (10)
60	698	707	13.44	65.16	5.11	1.82	β C5-C6-C1 (13) + β C6-C1-C2 (13) + β C3-C2-N10 (11)
61		687	7.19	12.52	4.57	1.48	τ C17-C14-C12-C13 (11) + τ C19-C15-C13-C12 (10) + γ N27-C15-C17-C19 (16)
62		682	29.29	1.9	5.45	1.66	β O26-C24-C4 (14)
63		634	8.3	2.44	4.82	1.45	τ C5-C6-C1-C2 (13)+ γ O22-C4-C6-C5 (22)
64		624	65.89	20.81	2.91	0.76	τ H28-N27-C29-C31 (21)+ γ O30-C31-N27-C29 (14)

65		622	62.23	55.5	2.49	0.63	τ H28-N27-C29-C31 (25)+ γ O30-C31-N27-C29 (23)
66		565	4.06	11.38	6.19	1.55	ν C13-C12 (14) +β C17-C14-C12 (12) + β C15-C13-C12 (25) + β N11-C12-C14 (10)
67		525	21.37	1.48	2.79	0.57	τ H7-C1-C2-C3 (15) + τ C2-N10-N11-C12 (13) + γO22-C4-C6-C5 (14) + γ C24-C3-C5-C4 (10)
68		516	25.23	21.59	3.29	0.59	β O30-C29-C31 (26) + τ H28-N27-C29-C31 (11)
69		488	2.5	17.87	3.41	0.59	β N10-N11-C12 (12) + β N11-C12-C14 (12) + τ H28-N27-C29-C31 (11)
70		488	2.39	10.86	3.33	0.51	β O30-C29-C31 (29)
71		503	42.4	47.45	2.03	0.33	τ H28-N27-C29-C31 (25) + τ H34-C31-C29-N27 (13) + γ O30-C31-N27-C29 (20)
72		431	7.37	14.01	6.47	0.82	β O22-C5-C6 (38) + β O26-C24-C4 (19)
73		413	2.75	0.06	3.82	0.46	τ C4-C3-C2-C1 (37) + τ C5-C6-C1-C2 (10)
74		400	4.53	15.56	3.55	0.39	τ H16-C13-C15-C19 (11) + τ C15-C13-C12-C14 (18) + τ C19-C15-C13-C12 (23)
75		390	5.98	1.84	4.73	0.49	τ C17-C14-C12-C13 (18)
76		351	20.42	2.44	5.6	0.55	β O22-C5-C6 (13) + τ C17-C14-C12-C13 (13)
77		372	2.02	4.71	5.75	0.46	τ C6-C1-C2-N10 (16) +τ C5-C6-C1-C2 (20)+ γ C3-C1-N10-C2 (18) + γ N11-C13-C14-C12 (10)
78		331	26.98	1.02	8.52	0.76	ν N27-C19 (17) + β C31-C29-N27 (15) + β C19-C15-C13 (13)
79		277	10.88	3.69	4.16	0.3	β N27-C19-C17 (15) + β C31-C29-N27 (28)
80		274	3.46	0.67	2.78	0.14	τ H25-C24-C4-C3 (11) + τ O26-C24-C4-C3 (25)+ γ O22-C4-C6-C5 (10) + γ C24-C3-C5-C4 (36)
81		226	7.8	0.81	6.68	0.32	β C24-C4-C5 (37) + β O26-C24-C4 (11)
82		205	2	8.85	5.26	0.17	β C29-N27-C19 (20)
83		201	6.28	6.32	6.66	0.18	β C24-C4-C5 (28) + β N11-C12-C14 (13)
84		185	3.43	0.79	6.21	0.14	τ O26-C24-C4-C3 (27) + τ C6-C1-C2-N10 (10) + τ C1-C2-N10-N11 (19)
85		178	1.2	0.33	3.59	0.07	ν N10-C2 (11) + ν N11-C12 (10)

86		173	1.1	2.48	1.29	0.03	τ H33-C31-C29-N27 (26)
87		135	0.04	1.02	6.33	0.08	τ O26-C24-C4-C3 (15) + τ C6-C1-C2-N10 (25) + τ C4-C3-C2-C1 (12) + γ C24-C3-C5-C4 (18) + γ C3-C1-N10-C2 (11)
88		122	3.13	2.27	5.55	0.05	β C29-N27-C19 (18) + β N27-C19-C17 (11) + τ N10-N11-C12-C13 (10)
89		89	4.39	3.15	7.65	0.04	τ N10-N11-C12-C13 (11) + τ C29-N27-C19-C15 (21) + τ C31-C29-N27-C19 (17)
90		59	0.67	1.23	7.78	0.02	τ C6-C1-C2-N10 (11) + τ C15-C13-C12-C14 (11) + τ C31-C29-N27-C19 (24)
91		51	2.85	8.41	3.66	0.01	τ C29-N27-C19-C15 (46)
92		41	2.74	3.63	7.04	0.01	β C2-N10-N11 (17) + β N27-C19-C17 (10) + β N11-C12-C14 (15) + β N10-N11-C12 (21) + τ C31-C29-N27-C19 (13)
93		28	1.16	1.97	7.23	0	τ C15-C13-C12-C14 (15) + τ C2-N10-N11-C12 (26) + γ N11-C13-C14-C12 (20)
94		19	0.16	0.62	4.1	0	τ N10-N11-C12-C13 (40) + τ C1-C2-N10-N11 (39)

ν- stretching, β-in-plane, γ-out-of-plane bending, ω-wagging, t-twisting, δ-scissoring, ρ-rocking

Table No.3: Mulliken atomic charges and natural population analysis by B3LYP/6-311+G (d, p) methods for compounds 1 and 2

S.No	1			2		
	Atoms	Mulliken	NPA	Atoms	Mulliken	NPA
1	C1	0.2296	-0.1391	C1	0.2382	-0.1361
2	C2	-0.8255	0.0661	C2	-0.5961	0.0610
3	C3	-0.4565	-0.1180	C3	-0.6398	-0.1116
4	C4	1.1321	-0.2503	C4	1.1084	-0.2502
5	C5	-0.6605	0.3980	C5	-0.6602	0.4040
6	C6	-0.0751	-0.2503	C6	-0.0362	-0.2484
7	H7	0.1601	0.2332	H7	0.1614	0.2341
8	H8	0.1314	0.2205	H8	0.1360	0.2221
9	H9	0.1378	0.2227	H9	0.1413	0.2249
10	N10	0.0325	-0.2325	N10	0.0483	-0.2130
11	N11	0.0802	-0.2134	N11	0.0857	-0.2170
12	C12	-0.2336	0.0586	C12	-0.4281	0.0831
13	C13	-0.0079	-0.1477	C13	-0.0663	-0.1577
14	C14	-0.0040	-0.1674	C14	-0.0030	-0.1739
15	C15	0.0076	-0.2622	C15	-0.3265	-0.2271
16	H16	0.1289	0.2184	H16	0.1363	0.2224
17	C17	-0.2205	-0.2465	C17	0.1813	-0.2263

18	H18	0.1497	0.2286	H18	0.1514	0.2310
19	C19	-0.1347	0.1883	C19	0.0354	0.1710
20	H20	0.1085	0.2051	H20	0.1249	0.2127
21	H21	0.1083	0.2037	H21	0.1249	0.2137
22	N22	-0.3603	-0.7776	O22	-0.2576	-0.6524
23	H23	0.2343	0.3798	H23	0.3132	0.5047
24	H24	0.2345	0.3799	C24	0.2291	0.4165
25	O25	-0.2645	-0.6575	H25	0.1192	0.1321
26	H26	0.3116	0.5037	O26	-0.3213	-0.5854
27	C27	0.2645	0.4155	N27	-0.1937	-0.6287
28	H28	0.1175	0.1305	H28	0.2821	0.4041
29	O29	-0.3259	-0.5901	C29	0.0934	0.6879
30				O30	-0.3134	-0.6078
31				C31	-0.3884	-0.6729
32				H32	0.1657	0.2202
33				H33	0.1723	0.2261
34				H34	0.1817	0.2369

Table No.4: HOMO and LUMO energy, chemical potential, hardness and electrophilicity index calculated by B3LYP/6-311G (d, p) method for compounds 1 and 2

S.No	Parameters	1	2
1	E_{HOMO} (eV)	-5.7982	-6.3546
2	E_{LUMO} (eV)	-2.4644	-2.8674
3	$\Delta E=E_L-E_H$ (eV)	3.3338	3.4872
4	E_{HOMO-1}	-6.4294	-6.8258
5	E_{LUMO+1}	-2.1382	- 2.4666
6	$E_{HOMO-LUMO+1}$	4.29117	4.3592
7	Electro negativity χ	- 4.1313	-4.6110
8	Hardness (η)	1.6669	1.7436
9	Electrophilicity index(ω)	5.1197	6.0969
10	Softness (S)	0.2999	0.2867

Table No.5: The *ab initio* and DFT calculated electric dipole moment (debye), average Polaris ability (α_{tot} x10^{24}esu) and hyperpolarisability (β_{tot} x10^{30}esu) for compounds 1 and 2

S.No	Parameters	1	2
		Dipole moment	
1	μ_x	6.2266	-0.1444
2	μ_y	-0.6821	0.0574
3	μ_z	0.8041	0.3055
4	μ	6.3152	0.3428
		Polarisability	
5	α_{xx}	5.9885	-41.7691
6	α_{YY}	4.4032	28.2351
7	α_{ZZ}	-10.3028	13.5339
8	α_{XY}	-2.7671	0.025
9	α_{YZ}	6.0480	3.271
10	α_{yz}	-0.6480	0.047
11	α_0	0.02963	-3.300
12	$\Delta\alpha$	3.34	8.38
		Hyperpolarisability	
13	β_{xxx}	395	-187
14	β_{yyy}	-5.6801	2.6784
15	β_{zzz}	0.5058	2.0616
16	β_{xyy}	24.3304	34.582
17	β_{xxy}	-1.5201	52.145
18	β_{xxz}	44.2738	20.788
19	β_{xzz}	-23.437	1.9118
20	β_{yzz}	-2.1171	-6.7306
21	β_{yyz}	-0.9518	0.6259
22	β_{xyz}	-4.6389	-10.354
23	β_{tot}	398.42	159.737
24	β_0	3.44	1.38

Table No.6: Theoretically computed energies (a.u), zero-point vibrational energy (kcal/mol), rotational constants (Ghz), entropy (cal $mol^{-1}K^{-1}$) and dipole moment (Debye) for 1 and 2

S.No	Parameters	1	2
1	Total energies	-816.91	-969.60
2	Zero point energy	138.34	162.13
3	Rotational constants		
4		1.6877	1.18671
5		0.1387	0.08683
6		0.1282	0.08152
7	Entropy		
8	Total	124.96	143.16
9	Translational	42.34	42.82
10	Rotational	33.64	34.90
11	Vibrational	48.98	65.44
12	Dipole moment(D)	6.32	0.343

Table No.S1: Geometric bond lengths (Å), bond angles and dihedral angles (degree) of compounds 1 and 2 DFT-B3LYP/6-311+G(d,p)

Bond lengths	B3LYP/6-311+G (d, p)		Expt	Bond angles	B3LYP/6-311+G (d, p)		Expt	Dihedral angles	B3LYP/6-311+G (d, p)		Expt
	1	2			1	2			1	2	
C1-C2	1.414	1.414	1.368	N11-C12-C13	125.1	125.1		C3-C4-C27-H28	-0.015	-0.015	
C1-C6	1.380	1.378	1.393	C13-C12-C14	118.8	118.8	118.8	C3-C4-C27-O29/O26	179.988	179.988	
C1-H7	1.082	1.082	0.930	C12-C13-C15	121.0	121.0	121.1	C5-C4-C27-H28	179.978	179.978	
C2-C3	1.388	1.388	1.368	C12-C13-H16	118.4	118.4		C5-C4-C27-O29/O26	-0.019	-0.019	
C2-N10	1.412	1.411	1.446	C15-C13-H16	120.6	120.6		C4-C5-C6-C1	0.004	0.004	
C3-C4	1.404	1.402		C12-C14-C17	120.4	120.4		C4-C5-C6-H9	-179.997	-179.997	
C3-H8	1.085	1.085	0.930	C12-C14-H18	119.0	119.0		O22/O25-C5-C6-C1	179.999	180.0	
C4-C5	1.418	1.419		C17-C14-H18	120.6	120.6		O22/O25-C5-C5-H9	-0.002	-0.002	
C4-N27	1.454	1.454	1.3776	C13-C15-C19	120.3	120.3		C4-C5-O25-H26	-0.013	-0.013	
C5-C6	1.405	1.406		C13-C15-H20	120.1	120.1		C6-C5-O25-H26	179.992	180.0	
C5-O25	1.338	1.335	1.344	C19-C15-H20	119.6	119.6		C2-N10-N11-C12	179.970	179.970	−175.90
C6-H9	1.083	1.083		C14-C17-C19	120.9	120.9		N10-N11-C12-C13	179.885	179.885	
N10-N11	1.257	1.255	1.237	C14-C17-H21	119.9	119.9		N10-N11-C12-C14	-0.192	-0.192	3.2 0
N11-C12	1.406	1.412	1.4544	C19-C17-H21	119.2	119.2		N10-N11-C12-C15	-179.917	-179.917	-176.1
C12-C13	1.401	1.399		C15-C19-C17	118.6	118.6		N11-N12-C13-H16	-0.033	-0.033	
C12-C14	1.407	1.403	1.368	C15-C19-N22/N27	120.9	120.9		C14-C12-C13-C15	-0.011	-0.011	
C13-C15	1.386	1.386	1.401	C17-C19-N22/N27	120.4	120.4		C14-C12-C13-H16	-179.960	-179.960	
C13-H16	1.084	1.084	0.93	C19-N22-H23	117.4			N11-C12-C14-C17	-179.909	-179.909	
C14-C17	1.381	1.381		C19-N22-H24	117.4			N11-C12-C14-H18	0.050	0.050	
C14-H18	1.082	1.083	0.93	H23-N22-H24	113.9		121	C13-C12-C14-C17	0.012	0.012	
C15-C19	1.405	1.402		C5-O25-H26	107.8			C13-C12-C14-H18	179.971	179.971	
C15-H20	1.085	1.084	0.930	C4-C27-H28	116.1			C12-C13-C15-C19	-0.096	-0.096	

C17-C19	1.411	1.405		C4-C27-O29	124.2		124.5	C12-C13-C15-H20	179.743	179.743	
C17-H21	1.086	1.081	0.930	C27-H28-O29	119.7			H16-C13-C15-C19	179.852	179.852	
C19-N22	1.385		1.372	C4-C24-O26		124.2		H16-C13-C15-H20	-0.308	-0.308	
N22-H23	1.008		0.820	H25-C24-O26		119.7		C12-C14-C17-C19	0.094	0.094	
N22-H24	1.008		0.850	C19-N27-H28		109.5		C12-C14-C17-H21	-179.720	-179.720	
O25-H26	0.985			C19-N27-C29		109.5		H18-C14-C17-C19	-179.864	-179.864	
C27-H28		1.105		H28-N27-C29		109.5		H18-C14-C17-H21	0.322	0.322	
C27-O29		1.229	1.220	N27-C29-O30		120.2	123.37	C13-C15-C17-C19	0.197	0.197	
C19-N27		1.408	1.372	N27-C29-C31		119.9		C13-C15-C19-N22	177.723	177.723	
O22-H23		0.985		O30-C29-C31		119.9	121.44	H20-C15-C19-C17	-179.643	-179.643	
C24-H25		1.105		C29-C31-H32		109.5		H20-C15-C19-N22/N22	-2.117	-2.117	
C24-O26		1.228		C29-C31-H33		109.5		C14-C17-C19-C15	-0.198	-0.198	−0.5
N27-H28		1.012	0.903	C29-C31-H34		109.5		C14-C17-C19-N22/N27	-177.735	-177.735	−176.97
N27-C29		1.388	1.345	H32-C31-H33		109.5	109.5	H21-C17-C19-C15	179.618	179.618	
C29-O30		1.218	1.240	H32-C31-H34		109.5	109.5	H21-C17-C19-N22	2.081	2.081	
C29-C31		1.513	1.501	H33-C31-H34		109.5	109.5	C15-C19-N22-H23	161.677		
C31-H32		1.090	0.980					C15-C19-N22-H24	20.251		
C31-H33		1.093	0.980					C17-C19-N22-H23	-20.843		
C31-H34		1.090	0.980					C17-C19-N22-H22	-162.268		
Bond angles degree								C15-C19-N27-H28		-52.667	
C2-C1-C6	121.1	121.1	118.8	C6-C1-C2-N10	-179.982	-179.982		C15-C19-N27-C29		67.333	
C2-C1-H7	118.4	118.4		H7-C1-C2-C3	-179.998	-179.99		C17-C19-N27-H28		124.814	
C6-C1-H7	120.5	120.5		H7-C1-C2-N10	0.016	0.016		C17-C19-N27-C29		-115.186	

C1-C2-C3	118.7	118.7		C2-C1-C6-C5	-0.008	-0.008		C19-N27-C29-O30		-1.913	−4.0
C1-C2-N10	124.9	124.9	125.0	C2-C1-C6-H9	179.992	179.99		C19-N27-C29-C31		-178.087	-175.96
C3-C2-N10	116.4	116.4	116.5	H7-C1-C6-C5	179.993	179.99		H28-N27-C29-O30		-61.913	
C2-C3-C4	121.2	121.2		H7-C1-C6-H9	-0.007	-0.007		H28-N27-C29-C31		118.087	
C2-C3-H8	118.8	118.8		C1-C2-C3-C4	0.007	0.007		N27-C29-C31-H32		-67.609	
C4-C3-H8	120.0	120.0		C1-C2-C3-H8	179.992	179.99		N27-C29-C31-H33		52.391	
C3-C4-C5	119.4	119.4		N10-C2-C3-C4	179.994	179.99		N27-C29-C31-H34		172.391	
C3-C4-C27/C24	120.4	120.4		N10-C2-C3-H8	-0.021	-0.021		O30-C29-C31-H32		112.391	
C5-C4-C27/C24	120.3	120.3		C1-C2-N10-N11	-0.205	-0.205		O30-C29-C31-H33		-127.609	
C4-C5-C6	119.3	119.3		C3-C2-N10-N11	179.809	-179.81		O30-C29-C31-H34		-7.609	
C4-C5-O25/O22	122.0	122.0	124.5	C2-C3-C4-C5	-0.012	-0.012					
C6-C5-O25/O22	118.8	118.8		C2-C3-C4-C27/C24	179.982	179.98					
C1-C6-C5	120.3	120.3		H8-C3-C4-C5	-179.997	-179.99					
C1-C6-H9	121.3	121.3		H8-C3-C4-C27	-0.004	-0.004					
C5-C6-H9	118.4	118.4		C3-C4-C5-C6	0.006	0.006					
C2-N10-N11	115.2	115.2	113.4	C3-C4-C5-O25/O22	-179.989	-180.0					
N10-N11-C12	116.0	116.0	112.5	C24/C27-C4-C5-C6	-179.987	-180.0					
N11-C12-C13	116.2	116.2		C24/C27-C4-C5-O25/O22	0.018	0.018					

Table No.S2: Second order perturbation theory analysis of Fock matrix in NBO basis for compound 1 using B3LYP/6-311+G (d, p) method

S.No	Donar (i)	Occupancy (ED/e)	Acceptor (j)	$E^{(2)}$ kcal/mol	E_j-E_i kcal/mol	F(i, j) a.u.
1	π-C1-C6	1.7050	π*C2-C3	15.01	0.29	0.059
2	π-C1-C6	1.7050	π*C4-C5	24.42	0.27	0.075
3	π-C2-C3	1.6463	π*C1-C6	20.72	0.29	0.071
4	π-C2-C3	1.6463	π*N10-N11	20.62	0.24	0.065
5	π-C4-C5	1.5739	π*C2-C3	23.77	0.29	0.076
6	π-C4-C5	1.5739	π*C27-O29	26.49	0.25	0.078
7	π-N10-N11	1.9138	π*C2-C3	10.90	0.39	0.062
8	π-C12-C13	1.6099	π*N10-N11	23.94	0.23	0.068
9	π-C12-C13	1.6099	π*C14-C17	21.64	0.28	0.071
10	π-C14-C17	1.7296	π*C12-C13	15.01	0.29	0.061
11	π-C14-C17	1.7296	π*C15-C19	21.89	0.28	0.072
12	σ-C14-H18	1.9775	σ*C12-C13	25.91	1.08	0.06
13	LP(1) N11	1.9521	σ*C12-C14	30.85	0.96	0.08
14	LP(1) O25	1.9754	σ*C5-C6	38.53	1.13	0.022
15	LP(3) O25	1.5281	LP*(1)H26	528.65	0.64	0.520
16	LP(2) O29	1.8694	σ*-C27-H28	19.91	0.66	0.104
17	π*-C4-C5	0.4468	π*-C1-C6	139.31	0.02	0.082
18	π*-C4-C5	0.4468	π*-C2-C3	155.34	0.02	0.077
19	π*-N10-N11	0.2342	π*C2-C3	29.15	0.04	0.058
20	π*-N10-N11	0.2342	π*C12-C13	30.72	0.05	0.061
21	π*-C15-C19	0.4116	π*C14-C17	242.63	0.01	0.081
22	π*-C27-O29	0.1598	π*-C4-C5	128.73	0.02	0.074

Table No.S3: Second order perturbation theory analysis of Fock matrix in NBO basis for compound 2 using B3LYP/6-311+G (d, p) method

S.No	Donar	Occupancy	Acceptor	$E^{(2)}$ kcal/mol	E_j-E_i kcal/mol	F(i, j) a.u.
1	π-C1-C6	1.7057	π*C2-C3	15.00	0.29	0.059
2	π-C1-C6	1.7057	π*C4-C5	24.49	0.27	0.076
3	π-C2-C3	1.6423	π*C1-6	20.55	0.29	0.071
4	π-C2-C3	1.6433	π*C4-C5	15.23	0.27	0.058
5	π-C2-C3	1.6433	π*N10-N11	21.63	0.24	0.067
6	π-C4-C5	1.5692	π*C1-C6	11.78	0.29	0.055
7	π-C4-C5	1.5692	π*C2-C3	24.50	0.29	0.077
8	π-C4-C5	1.5692	π*C24-O26	26.05	0.26	0.078
9	π-N10-N11	1.9130	π*C2-C3	10.47	0.39	0.061
10	π-N10-N11	1.9130	π*C12-C13	10.28	0.40	0.062
11	π-C14-C17	1.6966	π*C12-C13	17.15	0.29	0.064
12	π-C14-C17	1. 6966	π*C15-C19	21.49	0.28	0.071
13	π-C15-C19	1.6375	π*C12-C13	22.57	0.29	0.073
14	π-C15-C19	1. 6375	π*C14-C17	16.51	0.29	0.063
15	LP(2) O22	1.7980	π*C4-C5	39.47	0.33	0.108

16	LP(2) O26	1.8689	σ*C24-H25	19.91	0.66	0.104
17	LP(1) N27	1.6837	π *C15-C19	25.15	0.28	0.076
18	LP(1) N27	1.6837	π*C29-O30	51.48	0.29	0.111
19	LP(2) O30	1.8683	σ*N27-C29	25.48	0.68	0.119
20	LP(2) O30	1.8683	σ*C29-C31	18.53	0.63	0.098
21	π*-C4-C5	0.4441	π*C1-C6	133.13	0.02	0.082
22	π*-C4-C5	0.4441	π*C2-C3	168.15	0.02	0.077
23	π*C15-C19	0.3891	π*C14-C17	255.37	0.01	0.081
24	π*C24-O26	0.1724	π*C4-C5	145.13	0.01	0.074

Table No.S4: Harmonic oscillator model of aromaticity DFT-B3LYP/6-311+G (d, p) calculated HOMA for compounds 1 and 2

S.No	Compound state	Component	EN	GEO	HOMA=1-EN-GEO
1	Neutral	HBA II	0.0134	0.0467	0.9400
		Aniline ring I	0.0126	0.0000	0.9874
		HBA II	0.0464	0.0467	0.9069
		Anilide ring I	0.0275	0.0310	0.9415
2	Anion	HBA II	0.0469	0.0467	0.9065
		Aniline ring I	0.0277	0.0311	0.9412
		HBA II	0.0471	0.0498	0.9032
		Anilide ring I	0.0212	0.0166	0.9622
3	Cation	HBA II	0.0470	0.0467	0.9063
		Aniline ring I	0.0277	0.0311	0.9412
		HBA II	0.0471	0.0498	0.9032
		ANILIDE I	0.0212	0.0166	0.9622

Table No.S5: DFT-B3LYP/6-311+G (d, p) method calculated NICS (ppm) values (neutral, cation and anion) compound 1

S.No	Bq	NICS (Aniline ring)					
		Neutral Isotropic	Neutral Anisotropic (zz)	Cation Isotropic	Cation Anisotropic (zz)	Anion Isotropic	Anion Anisotropic (zz)
1	-1.5	-5.7614	-18.0232	-3.5759	-10.6794	-4.7351	-15.3875
2	-1.0	- 7.7911	- 19.8244	-4.1301	-8.0875	-6.3020	-15.9395
3	-0.5	- 7.5206	- 11.8870	-2.3956	2.4636	-5.8955	-7.2306
4	0.0	- 6.2246	- 3.6437	-0.4899	10.4168	-4.8267	0.7887
5	0.5	- 7.6548	- 12.1987	-2.3974	2.4558	-6.0814	-7.9554
6	1.0	-7.9229	- 20.0740	-4.1298	-8.0905	-6.4256	-16.3414
7	1.5	- 5.8920	- 18.2550	-3.5744	-10.6776	-4.8533	-15.5983

S.No	Bq	NICS (HBA ring)					
		Neutral Isotropic	Neutral Anisotropic (zz)	Cation Isotropic	Cation Anisotropic (zz)	Anion Isotropic	Anion Anisotropic (zz)
1	-1.5	-6.1460	-17.6539	-4.3356	-0.4653	-2.8286	-8.4346
2	-1.0	-8.2307	-19.3215	-5.5896	-11.1032	-3.5489	-6.1229
3	-0.5	-8.1861	-11.7346	-4.3974	-1.5703	-2.7736	4.1803
4	0.0	-6.9995	-3.7044	-2.7295	6.1990	-1.6292	0.923
5	0.5	- 8.1809	-11.6672	-4.3817	-1.4696	-2.7778	4.2088
6	1.0	-8.2461	-19.3176	-5.5947	-11.0590	-3.5517	-6.0966
7	1.5	-6.1677	-17.6910	-4.5932	-12.5362	-2.8341	-8.4258

Table No.S6: DFT-B3LYP/6-311+G (d, p) calculated NICS (ppm) values (neutral, cation and anion) compound 2

S.No	Bq	NICS (Anilide ring)					
		Neutral Isotropic	Neutral Anisotropic (zz)	Cation Isotropic	Cation anisotropic (zz)	Anion Isotropic	Anion Anisotropic (zz)
1	-1.5	-7.4149	-21.0446	-3.8661	-11.4500	-4.2540	-3.6908
2	-1.0	-9.3526	-21.3086	-4.6940	-9.7752	-6.2305	-13.6105
3	-0.5	-8.1507	-11.6906	-3.1962	-0.3697	-5.3309	-5.0722
4	0.0	-7.1677	-7.3971	-0.9556	-9.6859	-4.4295	-1.8954
5	0.5	-8.8467	-17.1907	-2.5651	-2.4935	-6.5423	-5.6251
6	1.0	-8.3143	-21.7503	-4.3829	-8.5647	-7.0344	-14.0203
7	1.5	-5.7415	-17.9427	-3.8294	-11.3084	-4.8862	-13.8322

S.No	Bq			NICS (HBA ring)			
		Neutral Isotropic	Neutral Anisotropic (zz)	Cation Isotropic	Cation anisotropic (zz)	Anion Isotropic	Anion Anisotropic (zz)
1	-1.5	-5.7155	-16.7306	-3.7685	-11.4975	-5.3709	-11.8359
2	-1.0	-7.9439	-18.7802	-4.9698	-11.3972	*-6.007*	-7.1935
3	-0.5	-8.1732	-12.3367	–4.2540	-3.6908	-3.4624	-3.3755
4	0.0	-6.7806	-3.6606	-1.9203	-6.5351	-3.0128	-4.9087
5	0.5	-7.9095	-10.1136	-2.8484	-2.4266	-5.1205	-4.5348
6	1.0	-8.4613	-18.7292	-4.9139	-8.6267	-5.0539	-10.3224
7	1.5	-6.4465	-18.0699	-4.4773	-12.1345	-3.3966	-9.8291

Table No.S7: Calculated local reactivity properties of compound 1 using B3LYP/6-311+G (d, p) method for Mulliken derived charges

S.No	Atoms	fk^+	fk^-	Δfk(r)	sk^+	sk^-	sk^+/sk^-	Δsk (r)	$ωk^+$	$ωk^-$	Δωk(r)
1	C1	0.1174	0.0266	0.0908	0.0352	0.0080	4.4082	0.0272	0.6011	0.1364	0.4648
2	C2	-0.0178	-0.0749	0.0571	-0.0053	-0.0225	0.2381	0.0171	-0.0913	-0.3835	0.2922
3	C3	-0.0125	0.1164	-0.1289	-0.0038	0.0349	-0.1077	-0.0387	-0.0641	0.5958	-0.6599
4	C4	-0.0346	-0.0727	0.0382	-0.0104	-0.0218	0.4754	0.0114	-0.1770	-0.3724	0.1954
5	C5	0.1098	0.0587	0.0511	0.0329	0.0176	1.8699	0.0153	0.5619	0.3005	0.2614
6	C6	-0.0428	-0.0107	-0.0321	-0.0129	-0.0032	3.9901	-0.0096	-0.2194	-0.0550	-0.1644
7	N10	0.0794	0.0486	0.0308	0.0238	0.0146	1.6337	0.0092	0.4067	0.2489	0.1577
8	N11	0.0951	0.0252	0.0699	0.0285	0.0075	3.7796	0.0210	0.4869	0.1288	0.3581
9	C12	-0.0141	0.0706	-0.0847	-0.0042	0.0212	-0.2002	-0.0254	-0.0724	0.3615	-0.4339
10	C13	0.0111	-0.0320	0.0431	0.0033	-0.0096	-0.3467	0.0129	0.0568	-0.1639	0.2207
11	C14	0.0599	0.0382	0.0216	0.0180	0.0115	1.5650	0.0065	0.3064	0.1958	0.1106
12	C15	0.0109	-0.0110	0.0219	0.0033	-0.0033	-0.9872	0.0066	0.0556	-0.0563	0.1119
13	C17	-0.0002	-0.0190	0.0187	-0.0001	-0.0057	0.0126	0.0056	-0.0012	-0.0970	0.0958
14	C19	0.0687	0.1726	-0.1039	0.0206	0.0518	0.3981	-0.0312	0.3517	0.8835	-0.5318
15	N22	0.0329	1.0265	-0.9936	0.0099	0.3079	0.0320	-0.2980	0.1684	5.2552	-5.0868
16	O25	0.0651	0.0742	-0.0090	0.0195	0.0223	0.8780	-0.0027	0.3335	0.3798	-0.0463
17	C27	0.1012	0.0969	0.0044	0.0304	0.0291	1.0450	0.0013	0.5183	0.4960	0.0223
18	O29	0.0691	0.0494	0.0197	0.0207	0.0148	1.3993	0.0059	0.3540	0.2530	0.1010

Table No.S8: Calculated local reactivity properties using B3LYP/6-311+G (d, p) method for mulliken derived charges 2

S.No	Atoms	fk^+	fk^-	$\Delta fk(r)$	sk^+	sk^-	sk^+/sk^-	$\Delta sk\ (r)$	ωk^+	ωk^-	$\Delta\omega k(r)$
1	C1	0.0775	0.0593	0.0181	0.0222	0.0170	1.3056	0.0052	0.4724	0.3618	0.1106
2	C2	-0.0564	-0.1994	0.1430	-0.0162	-0.0572	0.2827	0.0410	-0.3437	-1.2158	0.8721
3	C3	-0.0018	0.1432	-0.1450	-0.0005	0.0411	-0.0126	-0.0416	-0.0110	0.8732	-0.8842
4	C4	-0.0124	0.1263	-0.1388	-0.0036	0.0362	-0.0985	-0.0398	-0.0758	0.7702	-0.8460
5	C5	0.0906	0.0856	0.0050	0.0260	0.0245	1.0581	0.0014	0.5522	0.5218	0.0303
6	C6	0.0098	-0.0997	0.1095	0.0028	-0.0286	-0.0978	0.0314	0.0595	-0.6079	0.6673
7	N10	0.0974	0.1259	-0.0284	0.0279	0.0361	0.7742	-0.0082	0.5941	0.7673	-0.1733
8	N11	0.1057	0.1058	-0.0001	0.0303	0.0303	0.9992	0.0000	0.6446	0.6451	-0.0005
9	C12	-0.0372	-0.0426	0.0054	-0.0107	-0.0122	0.8739	0.0015	-0.2268	-0.2595	0.0327
10	C13	-0.0122	0.0149	-0.0272	-0.0035	0.0043	-0.8175	-0.0078	-0.0745	0.0911	-0.1656
11	C14	-0.0011	0.2137	-0.2148	-0.0003	0.0613	-0.0051	-0.0616	-0.0066	1.3031	-1.3097
12	C15	-0.2989	0.0370	-0.3358	-0.0857	0.0106	-8.0837	-0.0963	-1.8221	0.2254	-2.0475
13	C17	0.2486	-0.0035	0.2522	0.0713	-0.0010	-70.2141	0.0723	1.5159	-0.0216	1.5374
14	C19	0.2611	-0.1523	0.4133	0.0749	-0.0437	-1.7148	0.1185	1.5918	-0.9283	2.5201
15	O22	0.0594	0.0705	-0.0111	0.0170	0.0202	0.8424	-0.0032	0.3621	0.4298	-0.0677
16	C24	0.0646	-0.0178	0.0823	0.0185	-0.0051	-3.6340	0.0236	0.3936	-0.1083	0.5019
17	O26	0.0534	0.0484	0.0050	0.0153	0.0139	1.1027	0.0014	0.3255	0.2952	0.0303
18	N27	0.0121	0.0083	0.0038	0.0035	0.0024	1.4581	0.0011	0.0737	0.0506	0.0232
19	C29	0.0124	0.0995	-0.0871	0.0036	0.0285	0.1245	-0.0250	0.0755	0.6065	-0.5310
20	O30	0.0685	0.0850	-0.0165	0.0196	0.0244	0.8056	-0.0047	0.4177	0.5184	-0.1008
21	C31	-0.0128	-0.0182	0.0054	-0.0037	-0.0052	0.7043	0.0015	-0.0783	-0.1112	0.0329

Table No.S9: Calculated maximum absorption wavelength of compound 1 in various solvents

S.No	Solvent	ΔE (eV)	f (a.u)	λ_{max} (nm)	Types of transition	% of transition
1	Benzene	2.7322	0.0001	453.79	H-1 →L+1	22.47
		2.9177	0.4659	424.94	H → L+1	2.26
		3.2235	0.7292	384.63	H → L+1	96.16
2	Chloroform	2.7495	0.0001	450.93	H-1 →L+1	21.49
		2.8981	0.4496	424.94	H → L+1	2.91
		3.2118	0.7267	384.63	H → L+1	95.54
3	Dichloromethane	2.7597	0.0001	449.27	H-1 →L+1	20.58
		2.8885	0.4503	427.82	H → L+1	3.20
		3.2057	0.7177	386.03	H → L+1	95.25
4	Acetone	2.7681	0.0001	447.91	H-1 →L+1	19.80
		2.8883	0.4298	429.24	H → L+1	4.06
		3.2097	0.7184	386.76	H → L+1	94.37
5	Ethanol	2.7691	0.0001	447.74	H-1 →L+1	19.68
		2.887	0.4325	429.38	H → L+1	4.19
		3.2085	0.7162	386.24	H → L+1	94.40
6	Methanol	2.7709	0.0001	447.45	H-1 →L+1	19.54
		2.8898	0.4185	429.05	H → L+1	4.51
		3.2129	0.7203	385.9	H → L+1	93.92

7	Acetonitrile	2.771	0.0001	447.44	H-1→L+1	19.50
		2.8875	0.4266	429.38	H → L+1	4.28
		3.21	0.7167	386.24	H → L+1	94.15
8	Dimethyl sulphoxide	2.7707	0.0001	447.49	H-1 →L+1	19.41
		2.8781	0.4621	430.78	H → L+1	3.34
		3.1982	0.701	387.66	H → L+1	95.11
9	Water	2.7732	0.0001	447.08	H-1 →L+1	19.27
		2.887	0.4243	429.46	H → L+1	4.45
		3.2104	0.7153	386.43	H → L+1	93.97
		3.1982	0.701	387.66	H → L+1	95.11

Table No.S10: Calculated and experimental maximum absorption wavelength of compound 2 in various solvents

S.No	Solvent	ΔE (eV)	f (a.u)	λ_{max} (nm)	Types of transition	% of transition	Experimental absorption maximum (nm)
1	Water	2.6898	0.0001	460.94	H-1 → L	92.89	
		3.1133	0.9654	398.24	H → L	99.09	
		3.453	0.3084	359.06	H → L+1	95.76	359
2	Ethanol	2.6873	0.0001	461.37	H-1 → L	92.83	
		3.1094	0.9756	398.74	H → L	99.15	
		3.45	0.3067	359.37	H → L+1	95.84	358.9, 245
3	Acetonitrile	2.6885	0.0001	461.17	H-1 → L	92.86	
		3.112	0.9692	398.41	H → L	99.11	
		3.4517	0.3081	359.2	H → L+1	95.79	357.2, 241.3
4	Acetone	2.6867	0.0001	461.47	H-1 → L	92.81	
		3.1103	0.9741	398.63	H → L	99.14	
		3.4499	0.3076	359.39	H → L+1	95.84	360.14
5	Dichloromethane	2.6815	0.0001	462.37	H-1 → L	92.68	
		3.1014	0.9967	399.77	H → L	99.24	
		3.4436	0.3034	360.05	H → L+1	96.01	355.37, 243.17
6	Chloroform	2.6755	0.0001	463.4	H-1 → L	92.52	
		3.1013	1.001	399.78	H → L	99.26	
		3.4397	0.3053	360.45	H → L+1	96.08	355.59
7	Benzene	2.6651	0.0001	465.22	H-1 → L	92.30	
		3.0981	1.0149	400.19	H → L	99.31	
		3.4329	0.3044	361.17	H → L+1	96.20	359.1
8	Dimethyl sulphoxide	2.6878	0.0001	461.28	H-1 →L	92.86	465sh,
		3.0986	0.9983	400.13	H → L	99.24	
		3.447	0.2988	359.69	H → L+1	95.95	371.68
9	Methanol	2.6886	0.0001	461.16	H-1 → L	92.85	
		3.1151	0.9623	398.01	H → L	99.07	
		3.4527	0.3104	359.09	H → L+1	95.75	257.2, 241.3

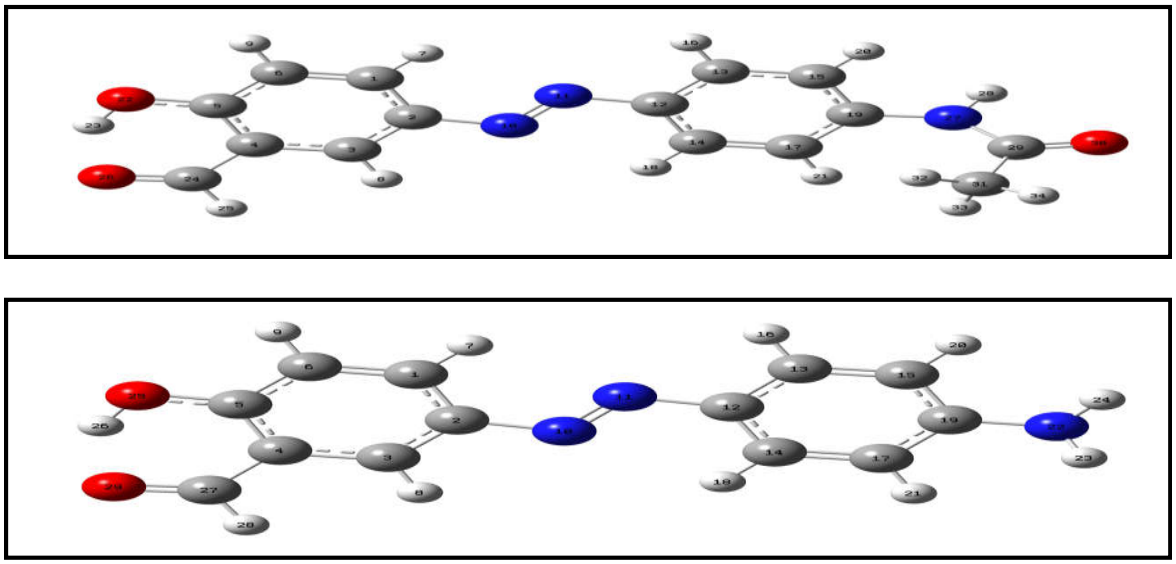

Figure No.1: Optimised structure of compounds 1 and 2

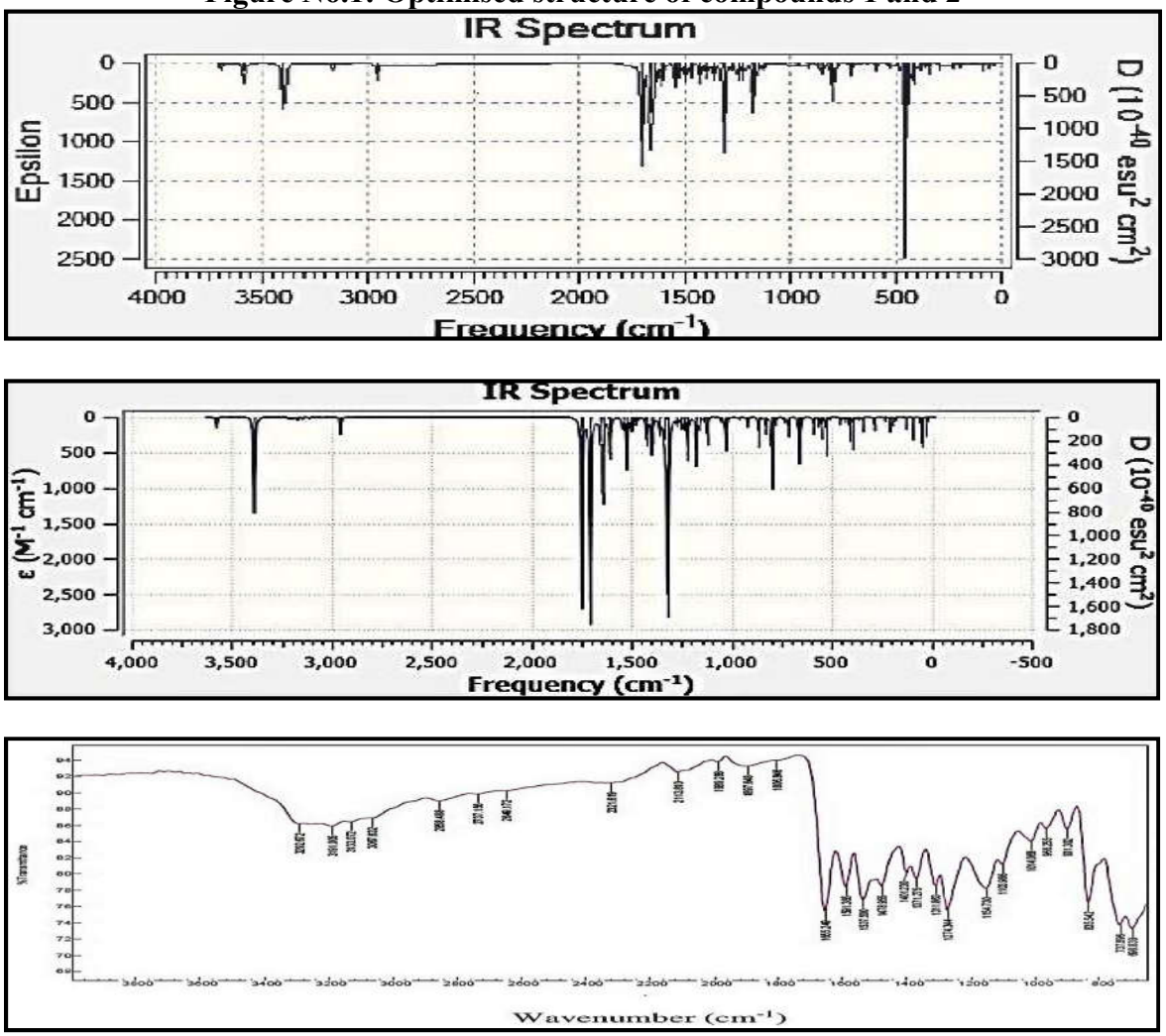

Figure No.2: Theoretical IR spectra of compounds 1 and 2 and experimental spectrum of compound 2 in KBr disc (cm^{-1})

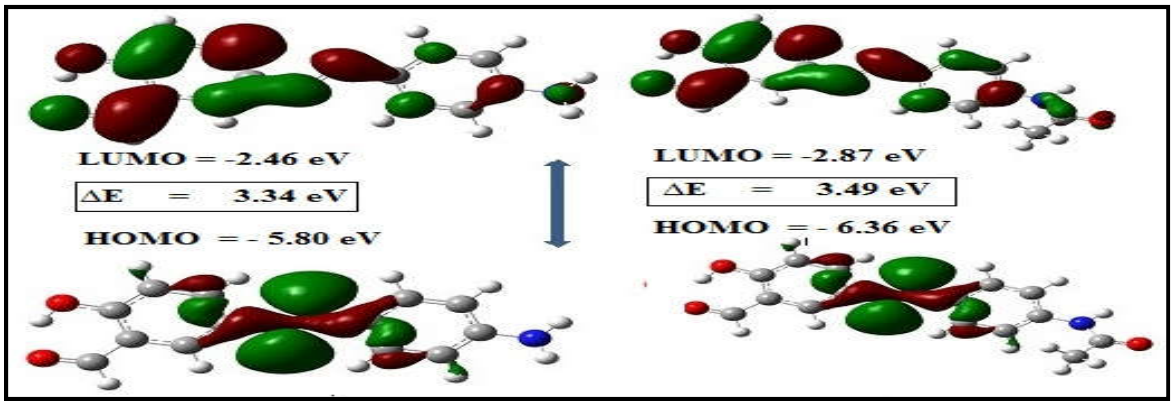

Figure No.3: MEP of compounds 1 and 2

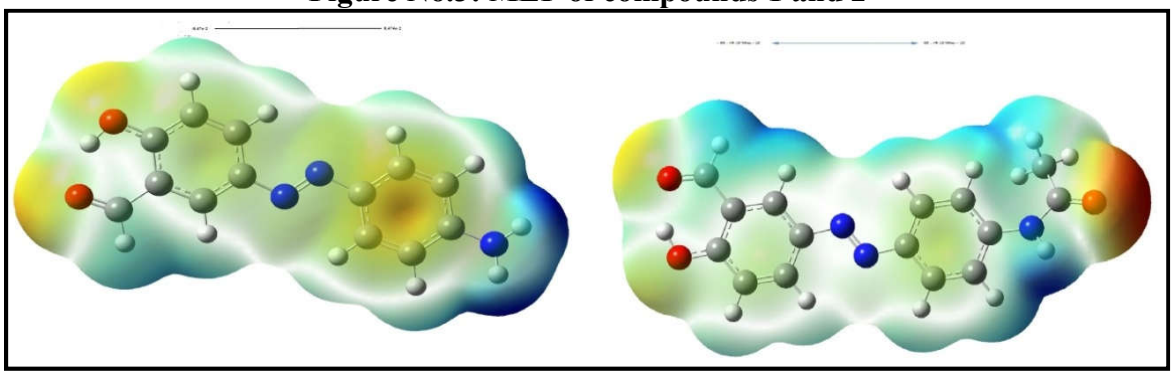

Figure No.4: HOMO-LUMO plots of compounds 1 and 2

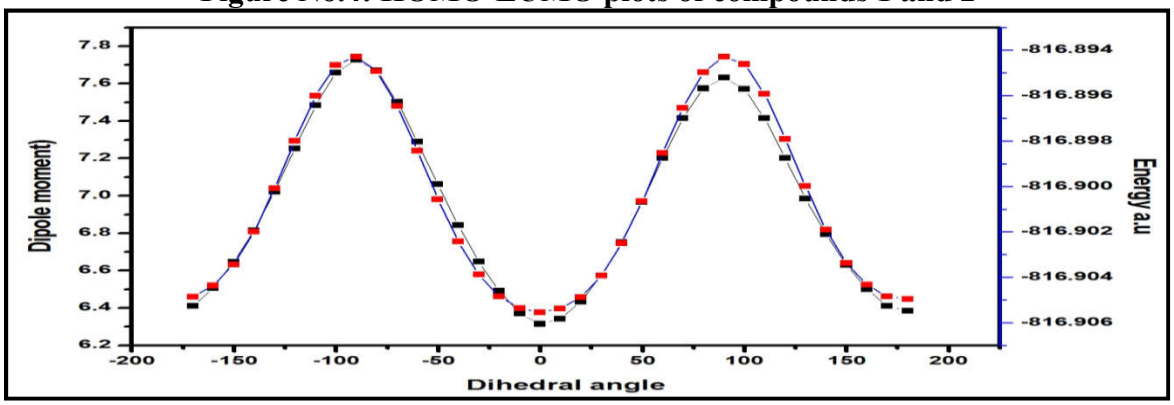

Figure No.S1: Variation of energy and dipole moment with dihedral angle (1, 2, 10, 11) for compound 1

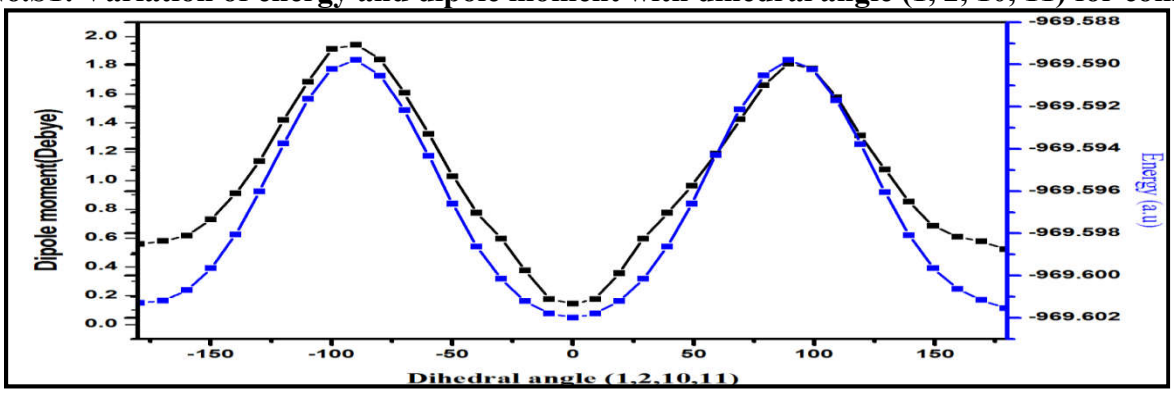

Figure No.S2: Variation of energy and dipole moment with dihedral angle (1, 2, 10, 11) for compound 2

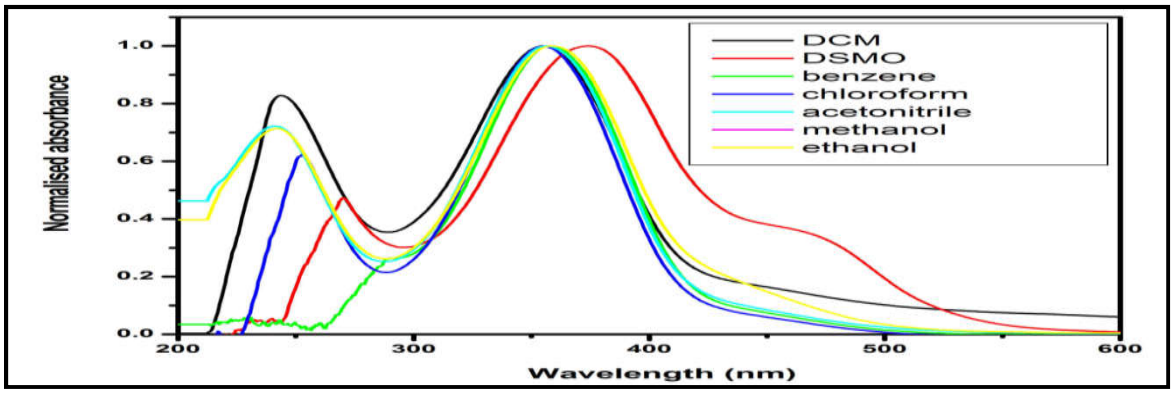

Figure No.S3: Absorption spectra of compound 2 at different solvents

CONCLUSION

In the present study, the optimized structural parameters of compounds 1 and 2 were obtained from DFT calculations. NBO analysis data shown that there are strong hyper conjugative interactions resulted in intra-molecular charge transfer causing stabilization of the title molecules 1 and 2. Non-linear optical behavior of the examined compounds were investigated by the determination of the electric dipole moment, the polarizability α and the hyperpolarizability β using the B3LYP method. The MEP shows the negative potential sites are located on oxygen atoms, while the positive potential sites are located around the hydrogen atoms. So, it's demonstrated that these compounds are often used as a NLO material. HOMO-LUMO energy gaps and implications of the electronic properties are examined. Additionally, the ionization potential (I), the electron affinity (A), the absolute electro negativity (v), the absolute hardness (g) and softness (S) parameters were obtained from HOMO–LUMO energies of the investigated molecule. HOMO→LUMO transition implies an electron density transfer to AZO groups to phenyl group.

ACKNOWLEDGEMENT

We are thanks to the Department of Chemistry, Annamalai University, Chidambaram for providing instruments facilities.

CONFLICT OF INTEREST

We declare that we have no conflict of interest.

BIBLIOGRAPHY

1. Zeitouny J, Aurisicchio C, Bonifazi D, De Zorzi R, Geremia S, Bonini M. Palma C A, Samori P, Listorti A, Belbakra A, Armaroli N. Photo induced structural modifications in multicomponent architectures containing azobenzene moieties as photo switchable cores, *J. Mater. Chem,* 19(27), 2009, 4715-4724.
2. Zollinger H. Color chemistry: Synthesis, properties and applications of organic dyes and pigments, *VCH, Wiley,* 2nd Edition, 1991, 496.
3. Slark A T, Hadgett P M. The effect of specific interactions on dye transport in polymers above the glass transition, *Polymer,* 40(14), 1999, 4001-4011.
4. Hallas Gand Choi J H. Synthesis and properties of novel aziridinylazo dyes from 2-amino-thiophenes, Part 2, Application of some disperse dyes to polyester fibers, *Dyes Pigments,* 40(2-3), 1999, 119-129.
5. Ho M S, Natansohn A and Rochon P. Azo polymers for reversible optical storage, 7, The Effect of the Size of the Photochromic Groups, *Macromolecules,* 28(18), 1995, 6124-6127.
6. Nabeshima Y, Shishido A, Kanazawa A, Shiono T, Ikeda T, Hiyama T. Synthesis of novel liquid-crystalline thiophene derivatives and evaluation of their photoresponsive behavior, *Chem. Mater,* 9(6), 1997, 1480-1487.

7. Iftime G, Labarthet F L, Natansohn A, Rochon P, Murti K. Main chain-containing AZO-tetraphenyldiaminobiphenyl photorefractive polymers, *Chem. Mater,* 14(1), 2002, 168-174.
8. Sharma G D, Suresh P, Sharma S.K and Roy M S. Photovoltaic properties of liquid-state photoelectrochemical cells based on PPAT and a composite film of PPAT and nanocrystalline titanium dioxide, *Synth. Met,* 158(12), 2008, 509-515.
9. Dirksen A, Zuidema E, Williams R M, De Cola L, Kauffmann C, Vogtle F, Roque A, Pina F. Photo activity and PH sensitivity of methyl orange functionalized poly (propyleneamine) dendrimers, *Macromolecules,* 35(7), 2002, 2743-2747.
10. Ikeda T and Tsutsumi O. Optical switching and image storage by means of azobenzene liquid-crystal films, *Science,* 268(5219), 1995, 1873-1875.
11. Gao A H, Li B, Zhang, Pei-Yu, Liu and Jianyong. Photochemical dynamics simulations for trans-cis photoisomerizations of azobenzene and bridged azobenzene, *Comput. Theor. Chem,* 1031, 2014, 13-21.
12. Feng Y. Photo-responsive perylene diimid-azobenzene dyad: Photochemistry and its morphology control by self-assembly, *Opt. Ma,* 30(6), 2008, 876-880.
13. Lee C H, Bihari B, Filler R and Mandal B K. New azobenzene non-linear optical materials for eye and sensor protection, *Opt. Mater,* 32(1), 2009, 147-153.
14. Papagiannouli I, Iliopoulos K, Gindre D, Sahraoui B, Krupka O, Smokal V, Kolendo A, Couris S. Third-order nonlinear optical response of push-pull azobenzene polymers, *Chem. Phys. Lett,* 554, 2012, 107-112.
15. Sudhir P, Ghosh G and Rout K. Synthesis and antimicrobial evaluation of some novel 4-hydroxy coumarin derivatives bearing AZO moiety, *Rasayan J. Che,* 6(2), 2013, 147-152.
16. Bae S, Freeman S and Shafei A E. Metallization of non-genotoxic direct dyes, *Dyes and Pigments,* 57(2), 2003, 121-129.
17. Sanjay T, Dinesh P, Manish P. *Saudi Pharm. Journal,* 15(1), 2007, 48.
18. Koshti M, Sonar P, Sonawane E. Synthesis of AZO compounds containing thymolmoiety, *Indian J. Chem,* 47(2), 2008, 329-340.
19. Phatok P, Jolly V S, Sharma K P. Synthesis and biological activities of some new substituted anyl AZO Schiff base, *Orient. J. Chem,* 16(1), 2000, 493-494.
20. Olcay B, Hakan B. Synthesis of schiff and mannich bases of isatin derivatives with 4-amino-4, 5-dihydro-1h-1, 2, 4-triazole-5-ones, *Molecules,* 13(9), 2008, 2126-2135.
21. Sharma K P, Jolly V S, Phatak P. Schiff bases and their derivatives as potential anticancer agents, *Ultra Scient. Phys. Sci,* 10, 1998, 263-266.
22. Majed H, Muzad, Talib, AL-Zamili F, Hyder K. Shanan. *J. Thi. Qar. Sci,* 1(2), 2008, 122-125.
23. FrischM J, TrucksG W, Schlegel H B, Scuseria G E, Robb M A, Cheeseman J R, Scalmani G, Barone V, Mennucci B, Petersson G A, Nakatsuji H, Caricato M, Li X, Hratchian H P, Izmaylov A F, Bloino J, Zheng G, Sonnenberg J L, Hada M, Ehara M, Toyota K. Gaussian 09 Revision D.01, *Gaussian Inc, Wallingford,* 2009.
24. Dennington R, Keith T, Millam J. Gauss. View, version 5.0; Semichem, *Inc.: Shawnee Mission, KS,* 2009.
25. Mauricio Alcolea Palafox. Scaling factors for the prediction of vibrational spectra, I. Benzene molecule, *Int. J. Quantum Chem,* 77(3), 2000, 661-684.
26. Michal H. Jamroz. Vibrational Energy Distribution Analysis VEDA4, *Warsaw,* 2004-2010, https://smmg.pl/software/veda.
27. Mohammed Bakir, Gabriel R Harewood, Alvin Holder, Ishmael Hassan, Tara Dasgupta, Paul Maragh P, Marvadeen Singh-Wilmot. 5-[(4-Methylphenyl) diazenyl] salicylaldehyde, *Acta Cryst,* 61(6), 2005, 1611-1613.
28. Hui-Fen Qian, Tao Tao. Crystal structures, solvatochromisms and DFT computations of

three disperse AZO dyes having the same azobenzene skeleton, *J. Mol. Str,* 1123, 2016, 305-310.
29. Mohammad Kazem Rofouei, Zahra Ghalami, Jafar Attar Gharamaleki, Giuseppe runo, Hadi Amiri Rudbari. *Acta Cryst. E,* 67, 2011, o1852.
30. Gunasekaran S, Thilak Kumar R, Ponnusamy S. Vibrational spectra and normal coordinate analysis of diazepam, phenytoin and phenobarbitone, *Spectrochim, Acta Part A,* 65(5), 2006, 1041-1052.
31. Krishnakumar V, John Xavier R. *Indian J. Pure and App. Phys,* l41, 2003, 597.
32. Pir H, Gunay N, Avci D, Atalay Y. Molecular structure, vibrational spectra, NLO and NBO analysis of bis (8-oxy-1-methylquinolinium) hydroiodide, *Spectro. Acta A,* 96, 2012, 916.
33. Ewa D. Raczynska, Malgorzata Hallman, Katarzyna Kolczynska, Tomasz M. Stępniewski. On the harmonic oscillator model of electron delocalization (HOMED) index and its application to heteroatomic π-electron systems, *Symmetry,* 2(3), 2010, 1485-1509.
34. Parr R G and Yang W. Density functional approach to the frontier-electron theory of chemical reactivity, *J. Am. Chem. Soc,* 106(14), 1984, 4049-4050.
35. Parr R G , Szentpaly L V, Liu S. Electrophilicity index, *J Am. Chem. Soc,* 121(9), 1999, 1922-1924.
36. Gumus H P, Tamer O, Avci D, Atalay Y. Quantum chemical calculations on the geometrical, conformational, spectroscopic and nonlinear optical parameters of 5-(2-Chloroethyl)-2, 4-dichloro-6-methylpyrimidine, *Spectrochim. Acta Part A: Molecular and Biomolecular Spectroscopy,* 129, 2014, 219-226.
37. Shaik S, Cohen S, Wang Y, Chen H, Kumar D, Thiel W. P450 enzymes: Their structure, reactivity and selectivity-modeled by QM/MM calculations, *Chem. Rev,* 110(2), 2010, 949-1017.
38. Siu F M, Che C M. Quantitative structure-activity (affinity) relationship (QSAR) study on protonation and cationization of α-amino acids, *J. Phys. Chem,* 110(44), 2006, 12348-12354.
39. Mohammed G. An Al-Khuzaie, Suaad M. H. Al-Majidi. Synthesis and characterization of new AZO compounds linked to 1, 8-naphthalimide as new fluorescent dispersed dyes for cotton fibers, *JPCS,* 1664, 2020, 1-17.

Please cite this article in press as: Thanikachalam V. *et al*. Experimental and DFT studies of (*E*)-5-((4-aminophenyl)-diazenyl)-2-hydroxyl-benzaldehyde and (*E*)-N-(4-((3-formyl-4-hydroxy-phenyl)diazenyl) phenyl) acetamide, *Asian Journal of Research in Chemistry and Pharmaceutical Sciences,* 10(2), 2022, 65-92.